PHILOSOPHICAL TRANSACTIONS OF THE ROYAL SOCIETY A MATHEMATICAL, PHYSICAL & ENGINEERING SCIENCES

Reliability of Structural Ceramics [and Discussion]

M. Knechtel, N. Claussen, J. Rodel, K. S. Kumar and R. Cahn

Phil. Trans. R. Soc. Lond. A 1995 **351**, 469-483
doi: 10.1098/rsta.1995.0047

Reliability of structural ceramics

By M. Knechtel[1], N. Claussen[1] and J. Rödel[2]

[1]*Advanced Ceramics Group,* [2]*Ceramics Group, Technische Hochschule Darmstadt, D-64295 Darmstadt, Germany*

In this study the influence of R-curve effects on reliability are investigated assuming natural flaws as being peripherally cracked spherical voids. Various experimental literature as well as own results are presented, including Al_2O_3, Si_3N_4, ZrO_2 and Al reinforced Al_2O_3.

1. Introduction

A variety of engineering ceramics can be used for structural applications such as silicon carbide for heat exchangers, silicon nitride for turbochargers, zirconia for extrusion dies and alumina for cutting tools. For their commercial use, good mechanical reliability and predictable performance is required, especially when designed for engine or turbine components where failure of a part may cause fatal damage of the whole device. Although numerous extrinsic and intrinsic reinforcing mechanisms have been developed to diminish the brittleness of ceramic materials the fracture toughness of most ceramics does not exceed values of 10 MP $am^{1/2}$. However, the application of sophisticated processing techniques, limiting typical flaw sizes and inhomogenities to a micrometre scale, allows attainment of high flexural strengths up in the GPa range. The limited resistance to crack propagation imparts a sensitive strength dependence of ceramics on defect population. Thus, in contrast to fracture toughness, strength is a statistical property which is mathematically described by the well-known Weibull distribution function. This article examines the efficiency of various reinforcing mechanisms in enhancing the reliability of structural ceramics.

2. Fracture mechanics background

(*a*) *Weibull distribution function*

Since the brittleness of ceramics implies that stress concentrations can not be relieved via plastic flow, the largest flaw is the failure site of the material. In this context, the fracture is induced by an applied stress that causes a stress intensity factor at the largest flaw higher than the critical value (K_{Ic}) of the material. Thus the most appropriate statistical description is the weakest link model, from which a three parametric strength distribution function, at first introduced by Weibull based on a heuristic approach (Weibull 1951), can be derived (Freudenthal 1968):

$$P(\sigma) = 1 - \exp\left\{-\left(\frac{\sigma - \sigma_u}{\sigma_0}\right)^m\right\}. \tag{2.1}$$

Phil. Trans. R. Soc. Lond. A (1995) **351**, 469–483
Printed in Great Britain

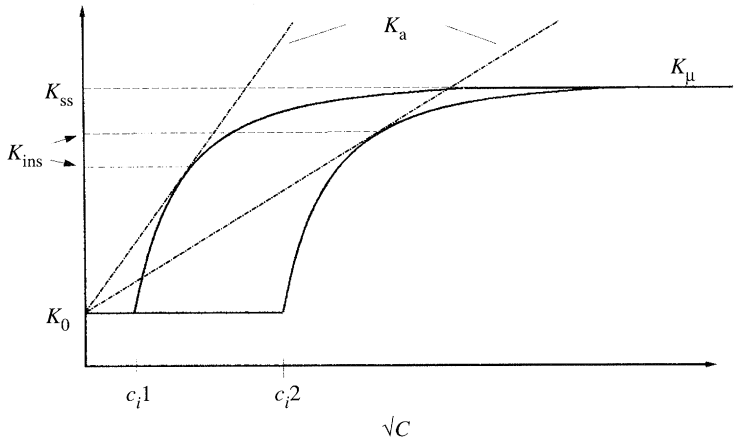

Figure 1. Schematical R-curves starting at two different penny-shaped cracks of length c_i1 and c_i2.

The probability of fracture (P) at a stress level (σ) is determined by the threshold stress (σ_u), below which no fracture occurs, a scaling parameter (σ_0) and a shape parameter (m). σ_0 is usually called the characteristic stress and m the Weibull modulus. In nearly all practical cases σ_u can be set to zero resulting in a two parametric distribution. Various numerical techniques can be applied (Bergmann 1986; Dortmanns & de With 1991; Steen *et al.* 1992) determining the shape and scaling parameter from a given number N of specimens tested with the maximum likelyhood method being the most reliable one. As an estimator (h_i) for the failure probability of ith ranked sample, a widely used and efficient expression is $(i - 0,5)/N$.

(*b*) *Influence of R-curve effects on strength variability*

It has been pointed out by previous authors that the existence of a rising crack-growth resistance, i.e. R-curve behaviour, leads to a narrowing of strength distribution (Cook & Clarke 1988; Shetty & Wang 1989). The basic mechanism reducing the effect of flaw size in R-curve materials is due to stable crack growth before fracture. Crack advancement occurs when the applied stress intensity (K_a) equals the crack tip toughness (K_0) which is independent on initial crack length c_i. However, the point of unstable propagation (K_{ins}), where the crack resistance of the material (K_μ) increases less than K_a with further crack extension, is shifted higher up the R-curve with increasing c_i (figure 1). Thus toughness at instability is increased with rising flaw size which imparts a diminished strength sensitivity on c_i. The impact of a rising crack resistance on strength distribution becomes less pronounced if the extent of stable crack growth is limited by a steep initial slope of the R-curve. The same is true for very shallow R-curves that reach their plateau value at extremely large crack lengths, which are far beyond the instability point.

Various experimental results support the fact that materials exhibiting pronounced R-curve behaviour reveal a narrow strength distribution. Improved flaw tolerability has been reported for transformation toughened zirconia (Kendall *et al.* 1987; Ready *et al.* 1993) which is well known for its crack-growth resistance. The dependence of strength distribution on R-curve has been pointed out for

ceria-stabilized zirconia (Pross *et al.* 1992) as well as magnesia-stabilized zirconia (Ramachandran *et al.* 1993). A significant reduction of Weibull modulus was observed when bend tests were carried out above the transformation temperature. A decrease of m from 92 down to a value of 9 was reported for Ce-TZP when tested at room temperature and 600 °C respectively (Hartsock & McLean 1984) and a reduction of a value of 20 in Mg-PSZ by a factor of 2 when tested at 400 °C (Ramachandran *et al.* 1993). Other examples are metal infiltrated ceramics where m is increased by a factor of two when compared to the porous preform (cf. ch. 4.4) or coarse-grained silicon nitride that exhibits higher m values when compared to the fine-grained material (Dressler 1993).

The following ceramic materials will be classified with respect to different mechanisms of strength control and the validity of these above mentioned correlations will be critically examined.

3. Theoretical evaluations and predictions

Determining the strength of a composite containing flaws requires the knowledge of flaw geometry, loading configuration and the stress–displacement relation of the reinforcing phase. As proposed by several authors (Evans & Davidge 1970; Rice 1984; Uematsu *et al.* 1993), natural flaws can be assumed as being spherical voids of radius r with a circumferential crack of length L (figure 2). For this case the fracture mechanical weight function under uniform loading conditions has been presented in the literature (Fett 1994). Besides the fact that experimental data can be reasonably well explained, it allows the accurate description of model composites containing spherical voids (Chao & Shetty 1992). Calculating the R-curve for an arbitrary stress-displacement relation of the reinforcing phase requires the knowledge of the crack opening displacement. This can be obtained from numerically solving an integral equation (Uematsu *et al.* 1993). In some special cases these integral equations exhibit a particularly simple form, especially if the bridging stresses remain constant at any crack length. Then an analytical expression for the crack resistance curve $K_\mu(c)$ can be derived:

$$K_\mu(c) = K_0 + p_{\max}\beta(c,r)\sqrt{\frac{2}{\pi}}\left(2\sqrt{(c-d)} + 0.4098\frac{\sqrt{(c-d)^3}}{c} + 0.1001\frac{\sqrt{(c-d)^5}}{c^2} + 1.4142(1-\beta(c,r))\frac{\sqrt{[(c+d)^2-(d+r)^2]}}{\sqrt{(c+r)}}\right), \tag{3.1}$$

$$\beta(a,r) = (1+c/r)^{-2}, \tag{3.2}$$

where K_0 is the crack tip toughness, $p_{\max}$ the closure stress and d the mean distance between the reinforcing elements, i.e. the crack length at which the R-curve starts from a pore of radius r. Usually the length of the circumferential crack is estimated to be of the order of a few grains (e.g. 10 μm).

For a typical monolithic alumina ceramic with a mean strength and fracture toughness of 400 MPa and 3.5 MP $am^{1/2}$ respectively, the application of Baratta's solution (Baratta 1981) for the stress intensity factor yields a value of 20 μm for r. Figure 3 shows resulting R-curves for an unbridged crack length of 5 μm in a range of crack lengths relevant for strength determination. The crack resistance curves were calculated for two bridging stresses. One R-curve is shown for a $p_{\max}$

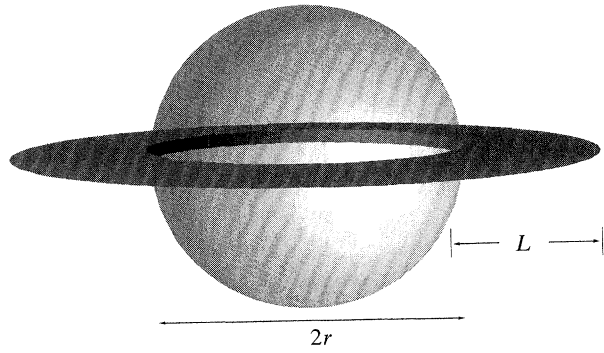

Figure 2. Natural flaw modelled as a spherical void of radius r and circumferential crack of length L.

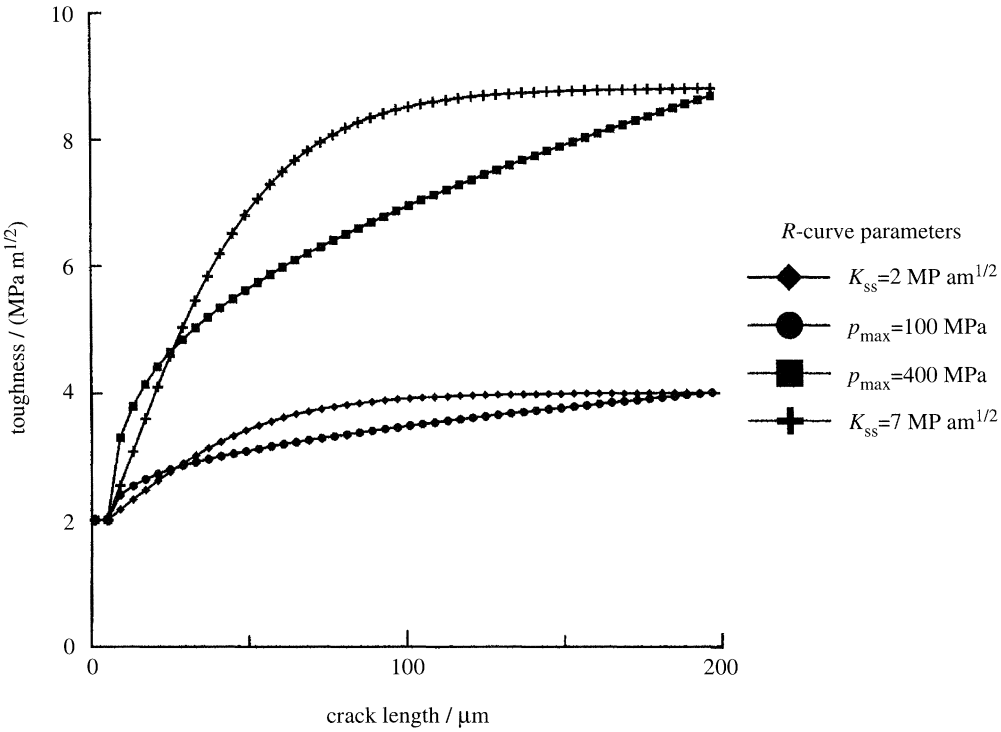

Figure 3. R-curves according to (3.2) (solid line) and (3.3) (solid line with rectangles) starting from a flaw as shown in figure 2 with radius of 20 µm and unbridged crack length of 5 µm.

of 100 MPa which corresponds to typical bridging stresses exerted by interlocking grains in alumina. Another crack resistance curve is shown for a bridging stress of 400 MPa, which results in a crack-growth resistance similar to silicon nitride (Schneider & Petzow 1994). The assumption of a Dugdale zone (i.e. constant bridging stresses) implies that the R-curve rises monotonically for any crack length. This can be used as a reasonable approximation, since some R-curve materials, like alumina, attain their steady-state toughness at a crack length far beyond the instability point. However, some materials such as silicon nitride can exhibit R-curves with very short bridging lengths where the plateau toughness is reached in the 100 µm range (Schneider & Petzow 1994). To take this fact into

account, a hypothetical R-curve was designed according to:

$$K_{\mathrm{hyp}}(c) = K_0 + K_{\mathrm{ss}} \tanh\left(\frac{c - c_{\mathrm{in}}}{c_{\max}}\right) \Phi(c - c_{\mathrm{in}}), \tag{3.3}$$

where K_{ss} is the steady-state toughness at the plateau of the R-curve, $c_{\max}$ a bridging length parameter, c_{in} the initial flaw size and Φ the Heavyside step function, which equals unity for positive and zero for negative arguments. The corresponding R-curves of (3.3) with plateau toughness of 2 and 7 MP am$^{1/2}$ are shown in figure 3.

For the monolithic material the dependence of strength on flaw size c is given by Griffith's equation:

$$\sigma_{\mathrm{b}} = Y K_{\mathrm{Ic}}/\sqrt{c}, \tag{3.4}$$

with K_{Ic} being the critical stress intensity factor and Y a numerical factor dependent on flaw geometry. Assuming strength being distributed according to the two parametric Weibull function and the peripheral crack length to be constant, the distribution of sphere sizes can be expressed as

$$P(r) = 1 - \exp[-(r_0/r)^{m/2}], \tag{3.5}$$

with r_0 being a characteristic radius. The numerical solution of the equations for unstable crack propagation,

$$K_{\mathrm{a}} = K_\mu \quad \text{and} \quad \frac{\mathrm{d}K_{\mathrm{a}}}{\mathrm{d}c} \geqslant \frac{\mathrm{d}K_\mu}{\mathrm{d}c}, \tag{3.6}$$

results in a strength distribution as depicted in figure 4, where the R-curves of (3.2) and (3.3) were used with the parameters according to figure 3. Included in this plot is the strength distribution for the unreinforced material. In the case of the material exhibiting a rising crack resistance the strength distribution shows a rather linear relation for limited R-curve effects, but deviation from the Weibull distribution becomes more pronounced for higher crack resistance. From the strength distributions for a set of 25 samples calculated with various bridging stresses, a linear regression was applied to obtain m and σ_0. The result of this calculation shows an increase of m and σ_0 with increasing bridging stresses and plateau toughness respectively (figure 5a, b). The R-curve for constant bridging stresses ($p_{\max}$) exhibits a steeper slope at short crack lengths making it less efficient in increasing reliability at low $p_{\max}$. However, when $p_{\max}$ rises above a certain value, e.g. 600 MPa, the amount of stable crack growth becomes less limited and the m values exceed even those of the hypothetical R-curve. In that regime the deviation from the Weibull distribution becomes more pronounced, making its applicability questionable. In a similar manner, the characteristic strength of the Dugdale type R-curve is lower than the one of the hypothetical R-curve but experiences a higher increase with closure stresses above 350 MPa. It should be pointed out that the absolut values for m and σ_0 depend on the special choice of the characteristic sphere radius r_0, e.g. the Weibull modulus at 600 MPa closure stresses is enhanced by roughly a factor of two when r_0 is increased from 20 to 30 μm, whereas the characteristic stress is reduced by 30%.

These results, which involve sample numbers common in testing on a laboratory scale may be insufficient from the manufacturer's point of view. Particularly in cases where large numbers of components are involved the probability of very

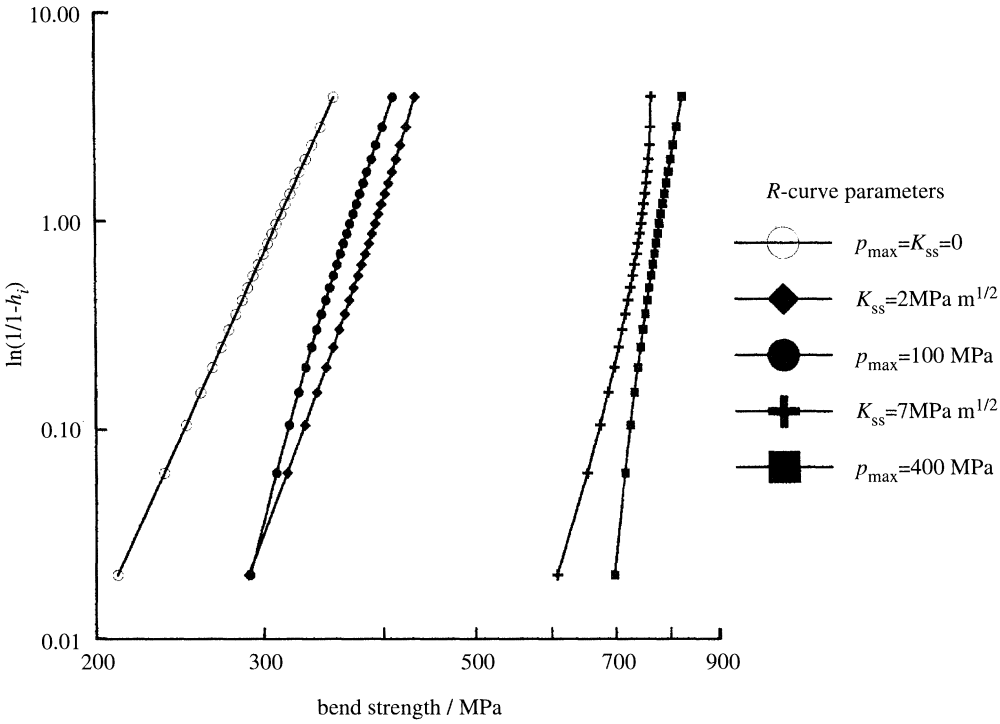

Figure 4. Strength distribution calculated for a sphere size distribution according to (3.4) without R-curve effects (open circles) and with R-curves of figure 3.

large flaw sizes increases. For these large flaws, instability occurs at large crack lengths where the R-curve flattens and does not lead to an effective strength enhancement. A calculation for fracture probabilities down to 1 in 10^7 demonstrates the deviation from the Weibull distribution (figure 6).

The fact that the slope of the strength values for the constant-bridging stress case is increased at low fracture probability is due to two facts. One is that the defect model of a peripherally cracked spherical void exhibits the deficiency that strength dependence on applied load is diminished asymptotically at high r/d ratios, i.e. for large pore radii if the circumferential crack length is kept constant (figure 7, where $r_{\max}$ corresponds to a fracture probability of 10^{-7}). The other is the monotonic increase of K_μ which leads to unrealistic crack lengths at instability.

4. Case studies

(*a*) *Alumina: defect controlled reliability*

The reliability and strength of monolithic alumina ceramics can be effectively improved with a large variety of advanced processing techniques, such as slip, pressure and centrifugal casting as well as numerous other sophisticated powder processing techniques. Due to mechanically interlocked grains, alumina exhibits rising crack resistance that increases with grain size (Chantikul *et al.* 1990) and achieves values as high as 6 MP am$^{1/2}$ at crack extensions of several millimetres (Steinbrech *et al.* 1990). Nevertheless no significant dependence of Weibull mod-

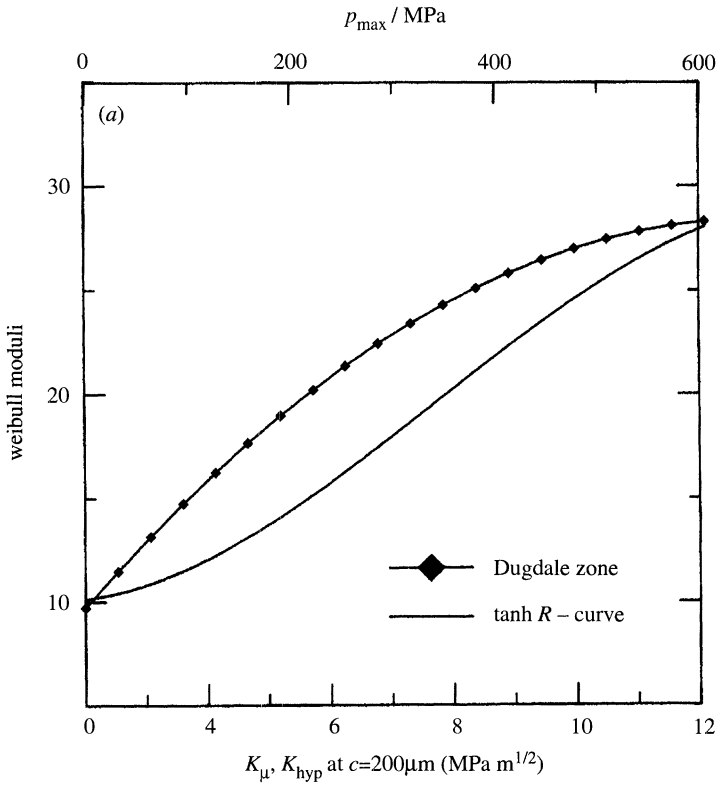

Figure 5. (*a*) Weibull moduli calculated for a set of 25 samples applying R-curves according to (3.2) and (3.3) as a function of crack resistance values at 200 μm crack length and closure stresses respectively.

ulus on grain size can be observed (figure 8) (Seidel *et al.* 1995). The R-curve of (3.2) was used by Seidel *et al.* to model the experimental results with reasonable agreement. Due to the moderate bridging stresses present in alumina (ranging between 30 and 120 MPa), the R-curve is too shallow to provide a significant narrowing of strength distibution.

(*b*) *Silicon nitride: defect/R-curve controlled reliability*

A relatively high fracture toughness value for silicon nitride containing rod-shaped grains was reported by Lange more than 20 years ago (Lange 1973). R-curve measurements on silicon nitride using radial indentation cracks have demonstrated that the toughness rises from 4.3 MP am$^{1/2}$ at a crack length of 50 μm to 9 MP am$^{1/2}$ at 600 μm for the particular material investigated (Li *et al.* 1992). Since fine-grained silicon nitride has a fracture toughness of 1.8 MP am$^{1/2}$, it was speculated that the crack tip toughness for the R-curve material may still lie well below 4 MP am$^{1/2}$ (Rödel 1992), which would necessitate a steeply rising crack resistance for the regime of very short cracks. Silicon nitride with strong R-curve should therefore be a prime candidate for low strength variability due to stable crack growth.

A frequently quoted result for a high Weibull modulus is described by Dressler (1993). In figure 9 the strength distribution for a fine grained silicon nitride (sin-

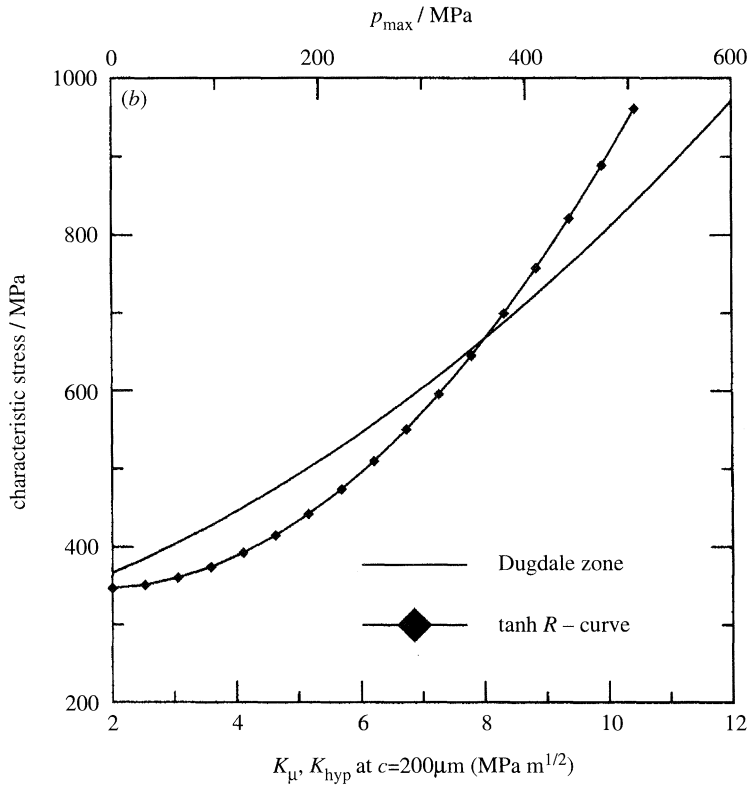

Figure 5. (*b*) Characteristic stresses calculated for a set of 25 samples applying *R*-curves according to (3.2) and (3.3) as a function of crack resistance values at 200 μm crack length and closure stresses respectively.

tered at 0.14 MPa N_2 for 20 min at 1780 °C and tempered at 1835 °C for 30 min at 10 MPa N_2) is compared to a coarse-grained silicon nitride (same sintering conditions, but tempering at 1900 °C for 6 h at 10 MPa N_2). The coarse-grained material has a very high Weibull modulus (46), but a comparatively low strength (902 MPa), whereas the fine-grained material has a mean strength of 1134 MPa and an m value of 14. The Weibull modulus appears to be a result of a general weakening of the material with the strongest specimen seeing a comparatively high strength reduction. This supposition is supported by the fact that the fracture origin in the fine-grained Si_3N_4 shifted from pores to large grains in the coarse-grained material (Dressler 1993). While an increasing grain diameter leads to an increase in steady-state toughness (Dressler 1993), but not in slope of the *R*-curve, we suggest that this increase in m with coarsening treatment is predominantly due to a change in defect population with a minor contribution arising from the change of *R*-curve behavior with microstructural scale.

(*c*) *Zirconia: plasticity/R-curve controlled reliability*

According to Swain & Rose (1989), transformation toughened zirconia shows either transformation or *R*-curve limited strength or a combination of both. A plot of strength versus peak toughness exhibits therefore a maximum at intermediate toughness values where the transformation has not lead to premature microcrack formation, but provides a strength enhancing steep *R*-curve (Swain & Rose 1989).

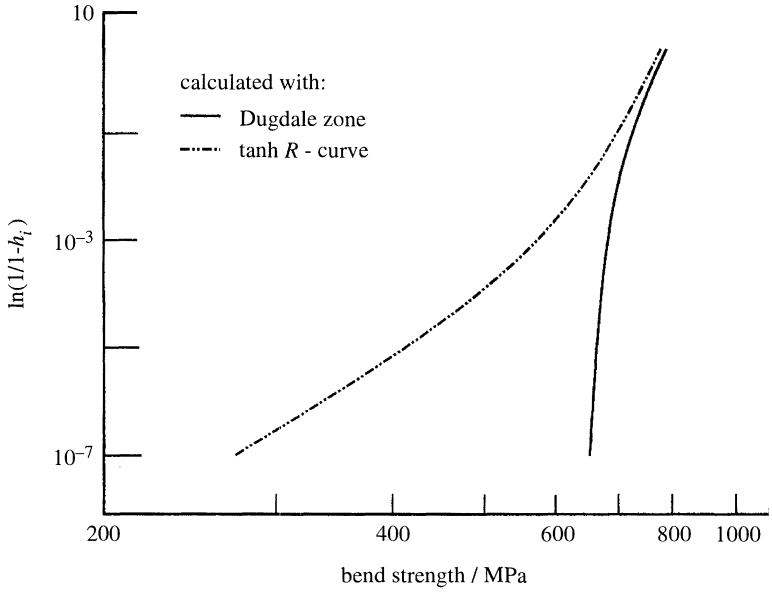

Figure 6. Strength distribution for a large set of samples corresponding to fracture probabilities down to 10^{-7}.

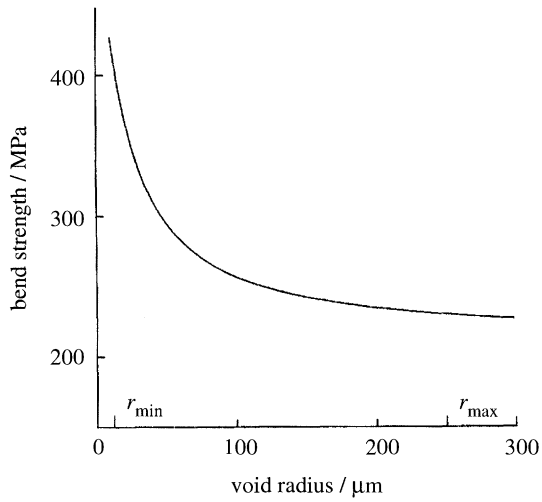

Figure 7. Dependence of strength on void diameter at a constant fracture toughness of 3.5 MP $am^{1/2}$ and circumferential crack length of 10 μm.

This duality can be followed in recent evaluations of the Weibull modulus for Ce-TZP at room temperature and 600 °C (where the chemical driving force for transformation is effectively reduced) as provided in figure 10 (Pross *et al.* 1992). In this case it is speculated that, at the critical transformation stress, microcrack formation begins and subsequent stable crack growth up the R-curve leads to high strength values as compared to the result obtained at 600 °C.

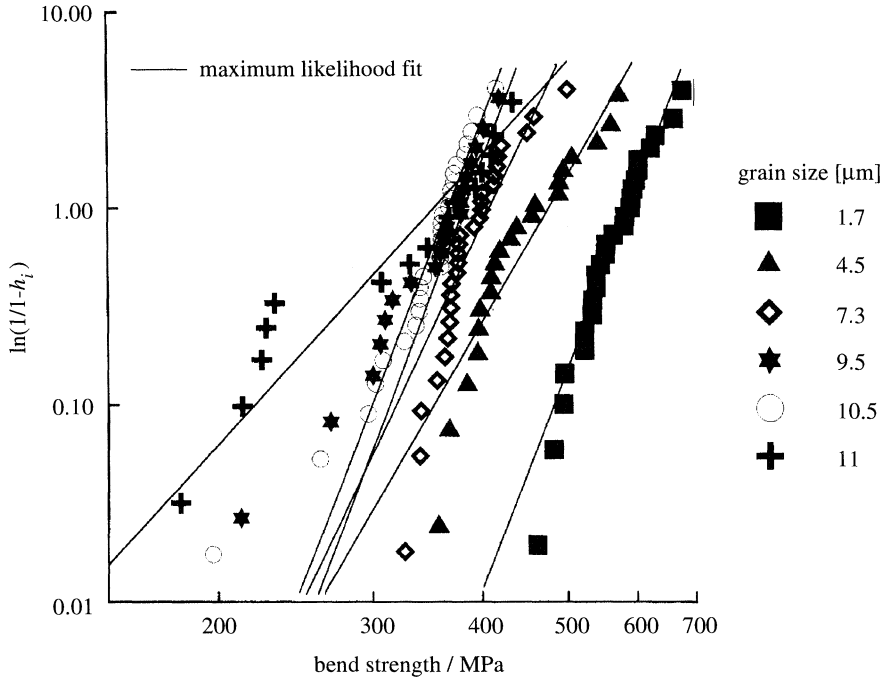

Figure 8. Strength distribution of alumina with various grain sizes.

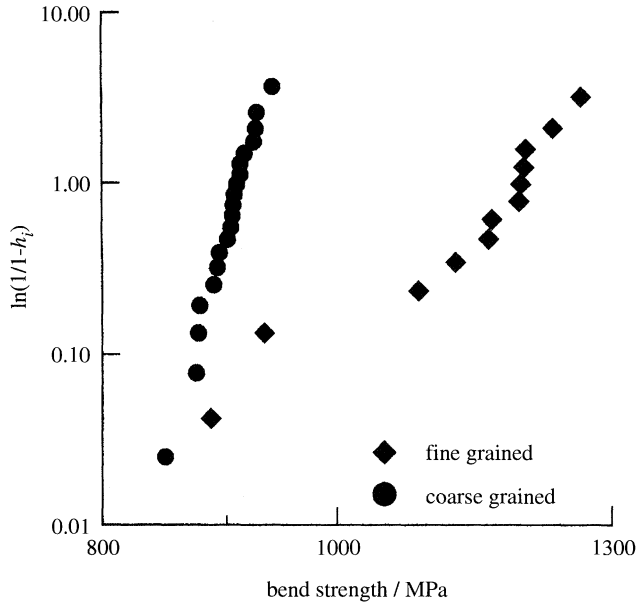

Figure 9. Strength distribution of silicon nitride with two different grain sizes (courtesy of W. Dressler).

(*d*) *Metal-reinforced ceramics: reduced flaw size/R-curve controlled reliability*

Various methods can be applied to fabricate metal-reinforced ceramics, such as squeeze casting (Lange *et al.* 1990), directed melt oxidation (Newkirk *et al.*

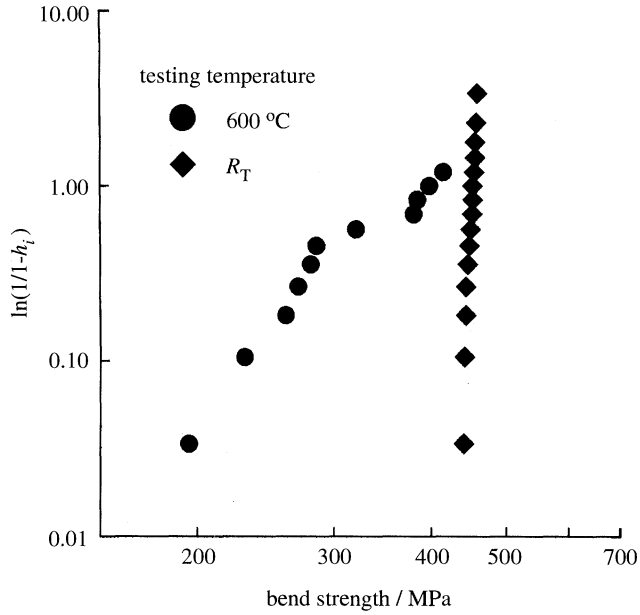

Figure 10. Strength distribution of Ce-stabilized zirconia at room temperature and 600 °C (Pross *et al.* 1992).

1986) and infiltration with (Travitzky & Claussen 1992) and without gas pressure (Toy & Scott 1990). Gas-pressure infiltration is successfully applied in a variety of metal–ceramic compositions including materials for high temperature applications like Ni_3Al–Al_2O_3 (Rödel *et al.* 1995). Porous ceramic preforms are obtained from sintering alumina green bodies to densities between 60 and 90% of theoretical density. The mechanical properties of the infiltrated composites are governed by metal content as well as microstructure (Priellip *et al.* 1995). The distribution of strength for three different microstructures (termed small (S), medium (M) and coarse (C)) of an Al–Al_2O_3 composite at a metal content of 25 vol% is depicted in figure 11, another for the medium microstructure at three different metal contents in figure 12. The Weibull moduli exhibit an increase by a factor of two when compared to the porous preforms for all cases except the one of the fine microstructure at 25 vol% metal content where no increase of m was observed. Due to the very small pore channel size of the preforms (0.08 μm), the stress–displacement relation of the metal ligaments bridging an advancing crack, reaches high closure stresses (Nohara 1982) at small crack openings, but is effective only up to an opening comparable to the ligament diameter (Ashby *et al.* 1989). Thus the resulting R-curve is believed to exhibit a very steep slope, therefore being ineffective in narrowing the strength distribution of the S composite. In contrast the coarse composite exhibits a mean pore channel size nearly an order of magnitude larger (0.75 μm) than the S composite, which imparts a more shallow R-curve thus resulting in reduced strength but enhanced reliability. Since the pore channel size remains essentially constant in the range of preform porosities applied, the shape of the crack resistance curve can be considered as being invariant of metal content. However, it has been demonstrated that K_{ss} is increased with metal content for a given microstructure, thus improving strength and narrowing strength distribution (figure 12).

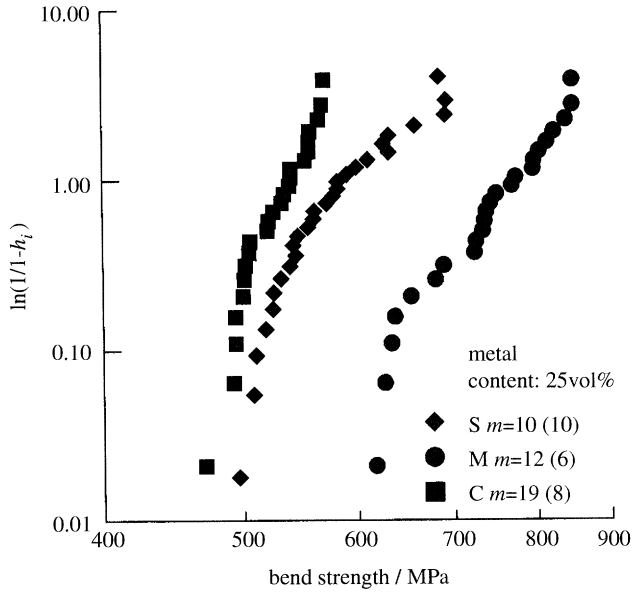

Figure 11. Strength distribution of Al infiltrated Al_2O_3 for three different microstructures. The values in parantheses correspond to the Weibull moduli of the uninfiltrated preforms.

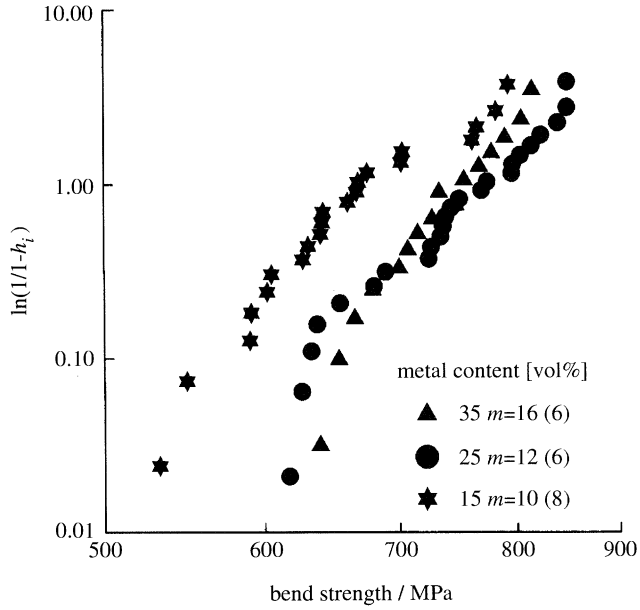

Figure 12. Strength distribution of an Al infiltrated Al_2O_3 with medium microstructure for three different metal contents. The values in parantheses correspond to the Weibull moduli of the uninfiltrated preforms.

Normalizing strength and toughness of all composites investigated so far to the data of the unifiltrated matrices revealed a higher increase in strength than toughness (Priellip *et al.* 1995). Thus a diminished flaw size in the infiltrated composites has to be taken into account. Assuming the largest pore or pore agglomerate being the fracture origin, this effect can be explained by the fact that

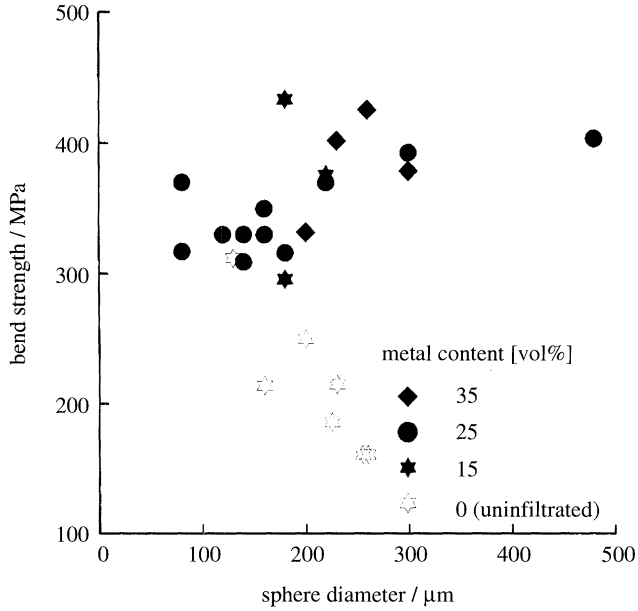

Figure 13. Strength of an Al–Al_2O_3 composite containing aluminium spheres of various diameter, acting as artificial flaws.

infiltrated pores act as single bridging elements. A further proof for this assumption can be given by the results of a model experiment, where bend bars with controlled defects were prepared incorporating polysterene spheres in the green body. The polymer was burned out during sintering and the specimens were subsequently infiltrated with metal. Figure 13 depicts the equatorial bend strength of an Al–Al_2O_3 composite where failure occured from the aluminium spheres for different metal contents and sphere diameters. No decrease in strength with increasing sphere diameter can be observed demonstrating the effectiveness of crack bridging. A more detailed analysis of strength distribution would therefore have to incorporate the effect of a rising crack resistance as well as the inhomogeneous distribution of bridging stresses.

5. Conclusions

It was demonstrated that reliability of structural ceramics can be controlled by at least four mechanisms with different degrees of efficiency, such as the distribution of defect size, *R*-curve effects, stress induced plasticity and reduced flaw size.

The influence of *R*-curve effects on strength distribution was modelled assuming natural flaws as being peripherally cracked spherical voids. For closure stresses in the range between 100 and 600 MPa, a maximum Weibull modul about three times higher than of the unreinforced reference case was predicted. Therefore the opportunity arises of further improving reliability through a combination of effective green forming techniques that narrow flaw size distribution with suitable crack-growth resistance imparting reinforcements.

The experimental data for strength and strength distribution presented were in the range of prediction except in the case of Ce-stabilized zirconia.

References

Ashby, M. F., Blunt, F. J. & Bannister, M. 1989 *Acta metall.* **37**, 1847–1857.

Baratta, F. I. 1981 *J. Am. Ceram. Soc.* C **64**, 3–4.

Bergmann, B. 1986 *J. Mater. Sci. Lett.* **5**, 591–619.

Chantikul, P., Bennison, S. J. & Lawn, B. R. 1990 *J. Am. Ceram. Soc.* **73**, 2419–2427.

Chao, L.-Y. & Shetty, D. K. 1992 *J. Am. Ceram. Soc.* **75**, 2116–2124.

Cook, R. F. & D. R. Clarke, D. R. 1988 *J. Am. Ceram. Soc.* **36**, 555–562.

Cox, B. N. & Marshall, D. B. 1994 *Acta metall. mater.* **42**, 341–363.

Dortmanns, L. J. M. G. & de With, G. 1991 *J. Am. Ceram. Soc.* **74**, 2293–2294.

Dressler, W. 1993 Ph.D. thesis, University of Stuttgart.

Evans, A. G. & Davidge, R. W. 1970 *J. nucl. Mater.* **5**, 314–325.

Fett, T. 1994 *Int. J. Fract.* **67**, R41–R47.

Freudenthal, A. M. 1968 In *Fracture* (ed. H. Liebowitz), vol. 2. Academic, 592–619.

Hartsock, D. L. & McLean, A. F. 1984 *Am. Ceram. Soc. Bull.* **63**, 266–270.

Kendall, K., McNAlford, N. & Birchall, J. D. 1987 *Mater. Res. Soc. Proc.* (ed. P. F. Becher, M. V. Swain & S. Somiya), vol. 78, p. 189. Pittsburgh: MRS Press.

Lange, F. F. 1973 *J. Am. Ceram. Soc.* **56**, 518–522.

Lange, F., Velamakanni, B. V. & Evans, A. G. 1990 *J. Am. Ceram. Soc.* **73**, 388–393.

Li, C.-W. & Yamanis, J. 1989 *Ceram. Engng Sci. Proc.* **10**, 632–645.

Li, C.-W., Lee, D.-J. & Lui, S.-C. 1992 *J. Am. Ceram. Soc.* **75**, 1777–1782.

Newkirk, M. S., Urquhart, A. W., Zwicker, H. R. & Breval, E. 1986 *J. Mater. Res.* **1**, 81–89.

Nohara, A. 1982 *Jap. J. appl. Phys.* **21**, 1287–1292.

Priellip, H., Knechtel, M., Claussen, N., Streiffer, S. K., Müllejans, H., Rühle, M. & Rödel, J. 1995 *J. Mater. Sci. Engng.* (In the press.)

Pross, J. 1992 Ph.D. thesis, MPI Stuttgart.

Pross, J., Schneider, G. A., Schubert, H. & Petzow, G. 1992 In *Verstärkung Keramischer Werkstoffe* (ed. N. Claussen). Oberursel: Informationsgesellschaft.

Ramachandran, N., Chao, L.-Y. & Shetty, D. K. 1993 *J. Am. Ceram. Soc.* **76**, 961–969.

Ready, M. J., McCallen, C. L., McNamara, P. D. & Lawn, B. R. 1993 *J. Mater. Sci.* **28**, 6748–6752.

Rice, R. W. 1984 *J. Mater. Sci.* **19**, 895–914.

Rödel, J. 1992 *J. Eur. Ceram. Soc.* **10**, 143–150.

Rödel, J., Prielipp, H., Sternitzke, M., Claussen, N., Alexander, K., Becher, P. & Schneibel, J. 1995 *Scr. metall.* (In the press.)

Schneider, G. A. & Petzow, G. 1994 *Key Engng Mater.* **89–91**, 563–568.

Seidel, J., Claussen, N. & Rödel, J. 1995 *J. Eur. Ceram. Soc.* **26**. (In the press.)

Shetty, D. K. & Wang, J.-S. 1989 *J. Am. Ceram. Soc.* **72**, 1158–1162.

Steen, M., Sinnema, S. & J. Bressers, J. 1992 *J. Eur. Ceram. Soc.* **9**, 437–445.

Steinbrech, R. W., Reichl, A. & Schaarwächter, W. 1990 *J. Am. Ceram. Soc.* **73**, 2009–2015.

Swain, M. V. & Rose, L. R. 1989 *J. Am. Ceram. Soc.* **69**, 511–518.

Toy, C. & Scott, W. D. 1990 *J. Am. Ceram. Soc.* **73**, 97–101.

Travitzky, N. & Claussen, N. 1992 *J. Eur. Ceram. Soc.* **9**, 61–65.

Uematsu, K., Sekiguchi, M., Kim, J.-Y., Saito, K., Mutoh, Y., Inoue, M. Fugino, M. & Miyamato, A. 1993 *J. Mater. Sci.* **28**, 1788–1792.

Weibull, W. 1951 *J. appl. Mech.* **18**, 293–297.

PHILOSOPHICAL TRANSACTIONS OF THE ROYAL SOCIETY A MATHEMATICAL, PHYSICAL & ENGINEERING SCIENCES

Discussion

K. S. Kumar (*Martin Marietta Laboratories, Baltimore, USA*). In the case-study relating to the intermetallic–infiltrated composite, Ni_3Al was selected as the intermetallic. Would it not be better to select a Ni-base superalloy or a refractory metal such as Nb or Ta to play the role that Ni_3Al is expected to, and realize significantly better improvements?

J. Rödel. A Ni-base superalloy will provide cavitation sites for premature cavity formation at the interface between intermetallic and ceramic if under tensile stress. Refractory metals will increase the density (as in Nb or Ta) of the composite.

R. Cahn (*Cambridge University, UK*). With regard to the experiments on alumina infiltrated with Ni_3Al minispheres, since weak alloy–ceramic interfaces were found, might I suggest two variants. (1) Try one of Liu's 'advanced aluminides', essentially Ni_3Al heavily alloyed with Cr, creating a higly oxidation-resistant intermetallic; this might bond better to alumina. (2) Try NiAl, which forms essentially an alumina layer on the surface when oxidized; indeed, it might be effective if it were to be preoxidized before infiltrating!

J. Rödel. We will try the Ni_3Al with Cr, since a strong bond is required for high strength. Experiments with NiAl are also planned, but of course we need a higher infiltration temperature still, which may technologically be not straightforward.

PHILOSOPHICAL TRANSACTIONS OF THE ROYAL SOCIETY A MATHEMATICAL, PHYSICAL & ENGINEERING SCIENCES

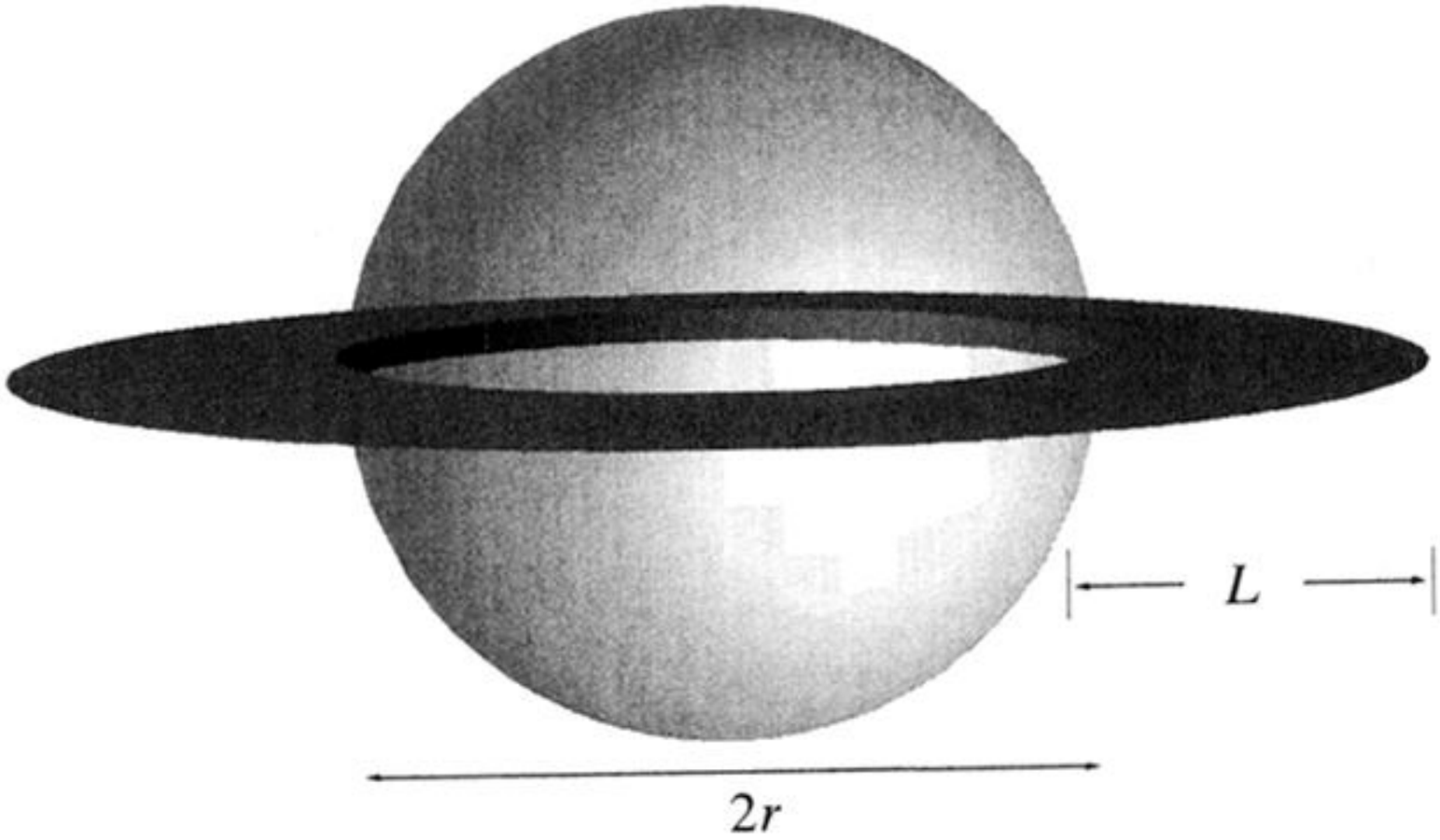

igure 2. Natural flaw modelled as a spherical void of radius r and circumferential crack of length L.